Morphology dependence of TiO$_2$ nanotube arrays on anodization variables and buffer medium[*]

Wen Xin(文鑫)[†], Cao Meng(曹萌), Wu Jie(吴杰), Tao Junchao(陶俊超), Sun Yan(孙艳), and Dai Ning(戴宁)[†]

(National Laboratory for Infrared Physics, Shanghai Institute of Technical Physics, Chinese Academy of Sciences, Shanghai 200083, China)

Abstract: Vertically oriented TiO$_2$ nanotube arrays were prepared by potentiostatic anodization of Ti foils in HF/acetic acid (HAC) aqueous solution. Anodization variables including anodization electrolyte concentration, anodization voltage, anodization time and buffer medium can be chosen and adjusted to manipulate the nanotube arrays to give the required length and morphology.

1. Introduction

Recently, vertically oriented TiO$_2$ nanotube arrays have received much attention due to their interesting properties and various applications in solar cells[1, 2], sensors[3], photocatalysis[4], and biomedicine[5]. Many routes have been tested to prepare TiO$_2$-based nanostructural materials, including templating synthesis[6], electrochemical lithography[7], photoelectrochemical etching[8], sol–gel[9], anodic oxidation[10, 11], etc. Anodic oxidation, a relatively simple and efficient technique, has been widely used and is easily automated to engineer TiO$_2$ porous and tubular structures. Moreover, some derivative methods have been used for the precise design and control of the geometrical features. For example, Gong and co-workers[12] have reported the growth of TiO$_2$ nanotubes to a length of about 500 nm and, subsequently, the lengths of nanotubes were increased to about 1000 μm by controlling the anodization electrolyte concentration[13]. Nageh and co-workers[14] have grown nanotubes using aqueous HCl electrolyte without fluoride. Yang and co-workers[15] prepared graded TiO$_2$ nanotubes by two-step anodization. TiO$_2$ thin film with aligned pores in the submicrometer and nanometer scales is of great interest in its use in photovoltaic cells due to its outstanding carrier transport capability. For instance, porous n-type TiO$_2$ films with a transparent p-type CuSCN filling the pores have been used to fabricate photovoltaic devices with a thin layer of CdS acting as the absorber[16]. Sun and co-workers[17] investigated TiO$_2$ nanotube photoelectrodes sensitized with CdS quantum dots for photoelectrochemical (PEC) solar cells. For these applications, the morphologies and structures of TiO$_2$ nanotubes are critical for high and reproducible cell efficiencies. The morphologies and structures of TiO$_2$ nanotube arrays are determined by some variables such as electrolyte concentration, pH value, anodization voltage, and electrolyte composition. In this work, we report the growth of TiO$_2$ nanotube arrays with their morphologies and structures being controlled by aqueous HF electrolyte solution and growth parameters. The addition of buffer electrolyte was useful to obtain a lower pH value in the pore bottom, which is helpful for the growth of TiO$_2$ nanotubes with varying sizes[18].

2. Experimental details

Prior to anodization, pure titanium foils (0.2 mm thick, 99.5%) were ultrasonically cleaned in acetone, and then rinsed with deionized water and dried in a nitrogen stream. The anodization was performed at room temperature in a two-electrode configuration with titanium foil as the working electrode and platinum gauze as the counter electrode. A DC anodizing power supply was used as the voltage source to drive the anodization and HF aqueous solution was used as the electrolyte solution. In addition, a buffer medium of HAC was added into the HF aqueous solution to reduce the dissolution rate of TiO$_2$ formed. The concentration of HF ranged from 0.3 wt% to 0.9 wt%, and the concentration of HAC varied from 2.5 wt% to 20 wt%.

3. Results and discussion

After the electrochemical process, the samples were rinsed by deionized water and dried in a nitrogen stream. Scanning electron microscopy (SEM) images of the TiO$_2$ nanotube films were taken on FESEM (field emission SEM, FEI Sirion 200). In this work, we used image analysis software (Image Pro Plus, by Media Cybernetics) to gather statistical parameters of the TiO$_2$ nanotubes from the SEM images. Figure 1 presents SEM images of the top and side views of the as-grown TiO$_2$ nanotube arrays. The mean area of the pore mouth of the nanotubes was calculated by a special function in the software. We set a certain intensity range to select the dark area of the SEM image and consequently both the gap between the tubes and the area of the pore mouth were selected. The gap can be abandoned by several restriction rules, such as area and roundness (see Fig. 1(a)). Then the statistics of the selected zones is provided automatically by the software. The length of nanotubes was measured directly by the software after spatial calibration (Fig. 1(b)).

Figure 2 displays the SEM image of TiO$_2$ nanotubes. Figures 2(a), 2(b), and 2(c) show the side, top, and bottom views
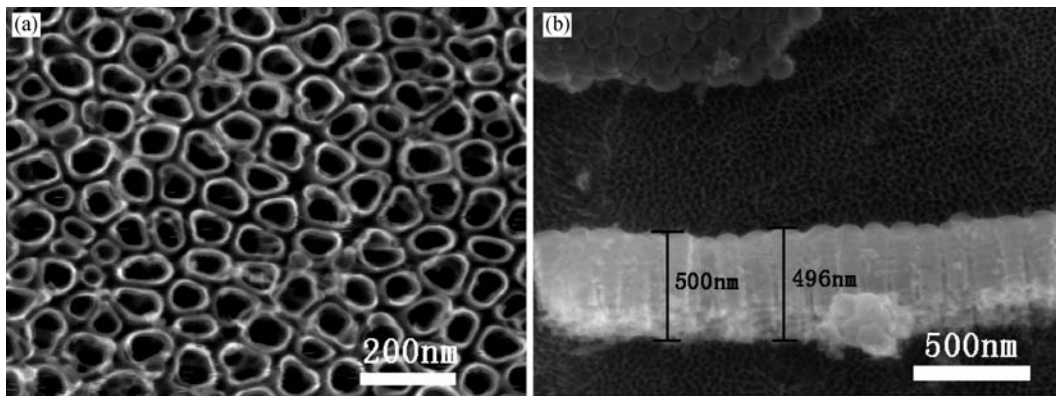
Fig. 1. SEM images of (a) top and (b) side views of TiO$_2$ nanotube arrays.
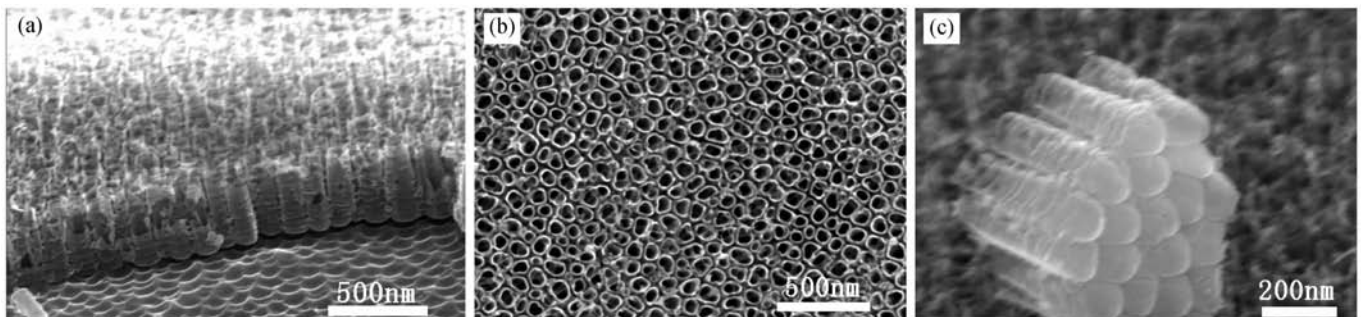

Fig. 2. Illustrative SEM images of (a) side, (b) top and (c) bottom views of TiO$_2$ nanotubes fabricated in 0.4 wt% HF solution at 20 V for 15 min.

of the nanotubes, respectively. Obviously, the individual nanotube looks like a test tube. The formation of nanotubes in fluoride-containing electrolytes is the result of three simultaneously occurring processes[18]: (1) field-assisted oxidation of the Ti metal that leads to the formation of the titanium dioxide film, (2) field-assisted dissolution of Ti metal ions into the electrolyte solution, and (3) chemical dissolution of Ti and TiO$_2$ due to etching away by fluoride ions. The formation of nanotubes in the aqueous-HF-containing electrolyte is described by the following two reactions:

$$Ti + 2H_2O \rightarrow TiO_2 + 4H^+, \qquad (1)$$

$$TiO_2 + 6HF \rightarrow [TiF_6]^{2-} + 2H_2O + 2H^+. \qquad (2)$$
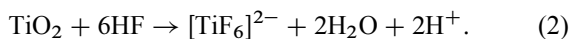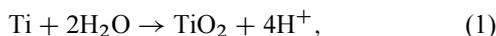
In the initial anodization, Ti metal oxidation dominates the reaction. The oxidation and hydrolysis of elemental titanium offer extra H$^+$, leading to the enhancement of localized acidification in the vicinity of the TiO$_2$ foil. The chemical dissolution rate of TiO$_2$ is strongly dependent on the pH value. If the anodization voltage can provide enough H$^+$, the chemical reaction in Eq. (2) will take place in the local area. This results in a higher field at the bottom of the pore that drives further oxidation and field-assisted dissolution accompanied by Ti ions coming out of the metal. The dissolution and breakdown of the bottom of TiO$_2$ pores occurs prior to the mouth due to the higher localized acidification. The metal substrate is exposed to the anodization electrolytes again after the bottom of the TiO$_2$ pores is dissolved into the electrolyte. The new layer of TiO$_2$ grows directly from the breakdown sites where it acts as the

new bottom of the already-formed TiO$_2$ pores. Thus, the same process of field-assisted formation and field-assisted dissolution of TiO$_2$ repeats subsequently to form porous TiO$_2$ thin films, with the TiO$_2$ pores growing more and more deeply into the Ti metal. In repeating the formation and dissolution process, the pore walls are conserved while the bottoms are destroyed by anodization electrolytes. If given enough anodization time, TiO$_2$ nanotubes will form with a configuration which looks like a conical flask and a rough side-wall. TiO$_2$ nanotube arrays were formed via self-organization of TiO$_2$, governed by the delicate balance of electrochemical oxidation of Ti into TiO$_2$. The nanotubes stop growing when the balance between electrochemical oxidation (at the pore bottom) and chemical dissolution of TiO$_2$ is established in the F$^-$-containing solution.

Figure 3 shows the growth process of TiO$_2$ nanotubes. Initially there are only TiO$_2$ pores on the surface of Ti metal substrate (Fig. 3(a)). Repeating the field-assisted formation and dissolution of TiO$_2$ leads to the pores growing wider and deeper into the substrate (Fig. 3(b)). Finally the development of TiO$_2$ pores results in TiO$_2$ nanotubes (Fig. 3(c)).

3.1. Effect of buffer medium on the microstructure of TiO$_2$ nanotube arrays

Figure 4 shows SEM images of TiO$_2$ nanotubes grown in aqueous solutions of 0.4 wt% HF at 20 V for 15 min without (Fig. 4(a)) and with (Fig. 4(b)) 20 wt% acetic acid (as the buffer medium in the anodization electrolyte). TiO$_2$ nanotubes were formed both in HF and in HF/HAC aqueous solutions at 20 V,
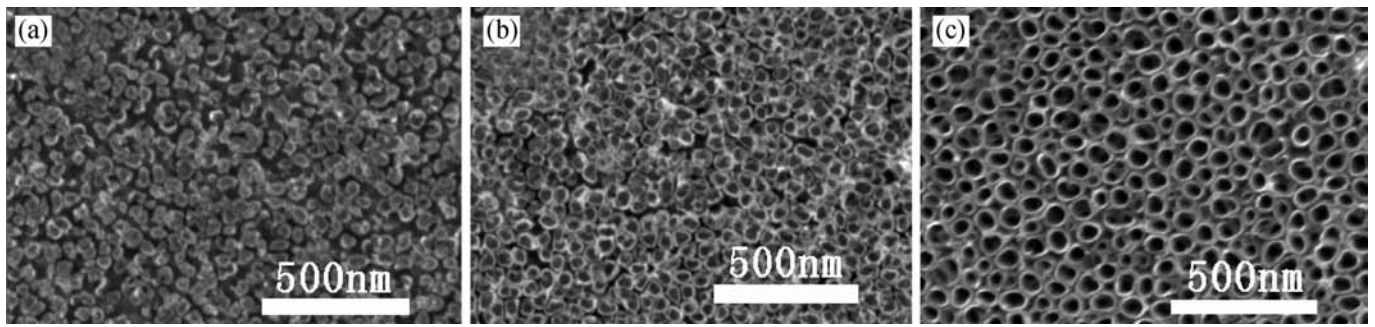
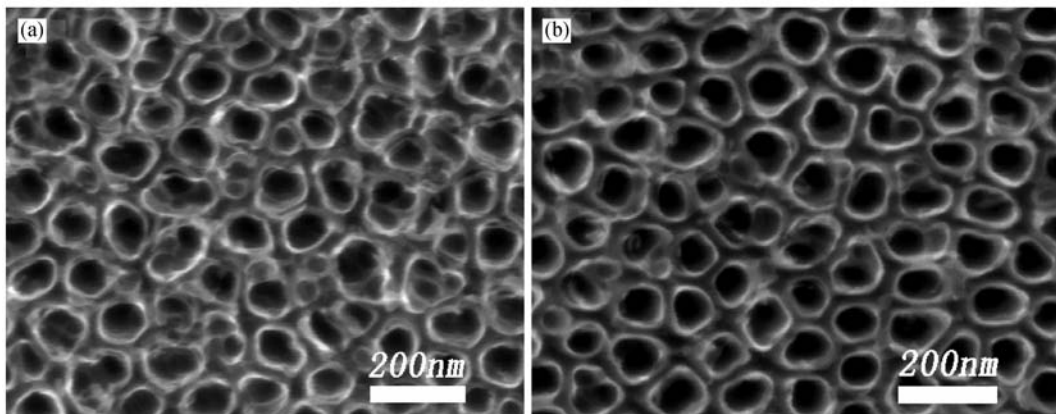Fig. 3. SEM top-surface images of (a) pore, (b) hole, and (c) nanotube.

Fig. 4. SEM top-view images of TiO$_2$ nanotubes obtained by anodization of Ti foil in 0.4 wt% HF at 20 V (a) without and (b) with acetic acid as the buffer medium in the anodization electrolyte.
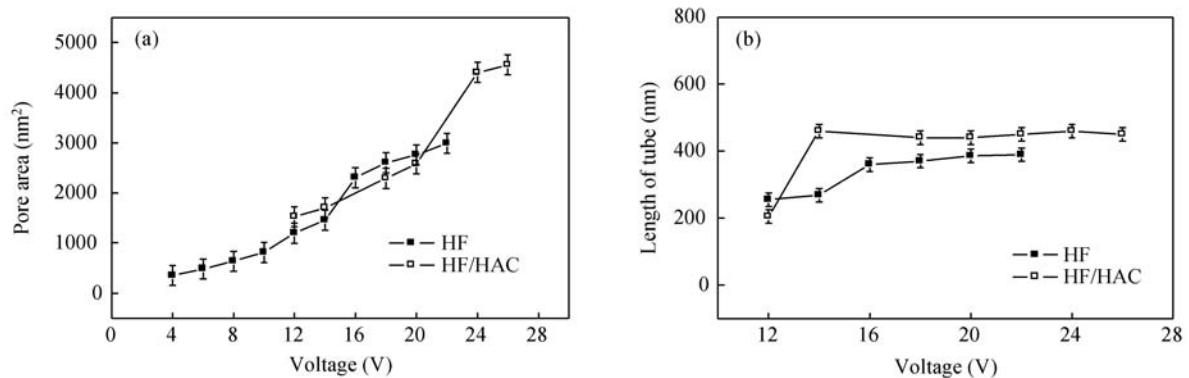

Fig. 5. Variation of (a) the mean area of the pore mouth and (b) length of TiO$_2$ nanotubes as a function of applied voltage for 15 min anodization using 0.4 wt% HF electrolyte with and without HAC as the buffer medium in the anodization electrolyte.

as verified in Fig. 4. There is no distinct difference between the size of TiO$_2$ nanotubes grown with and without acetic acid as the buffer medium. The nanotubes are 60 nm in inner diameter on average.

3.2. Effect of anodization voltage on the microstructure of TiO$_2$ nanotube arrays

Figure 5(a) plots the area of the pore mouth as a function of the anodization voltage in HF and HF/HAC (acetic acid) electrolytes anodized for 15 min. The mean area of the pore mouth becomes larger as the anodization voltage increases, indicating an increase in the pore diameter with increasing anodization voltage. The pores cannot grow when the anodization potential is under 4 V. On the other hand, the nanotubes become clogged when the anodization potential is higher than 22 V. Note that it seems that the presence of HAC in HF aqueous solution does not change the area of the pore mouth. However, both the minimum voltage for the initiation of TiO$_2$ nanotube growth and the highest voltage before the occurrence of clogging are increased.

Figure 5(b) displays the relationship between the nanotube length and the anodization voltage in HF and HF/HAC electrolytes for anodization carried out for 15 min. At low anodization voltage the length of TiO$_2$ nanotubes grown with
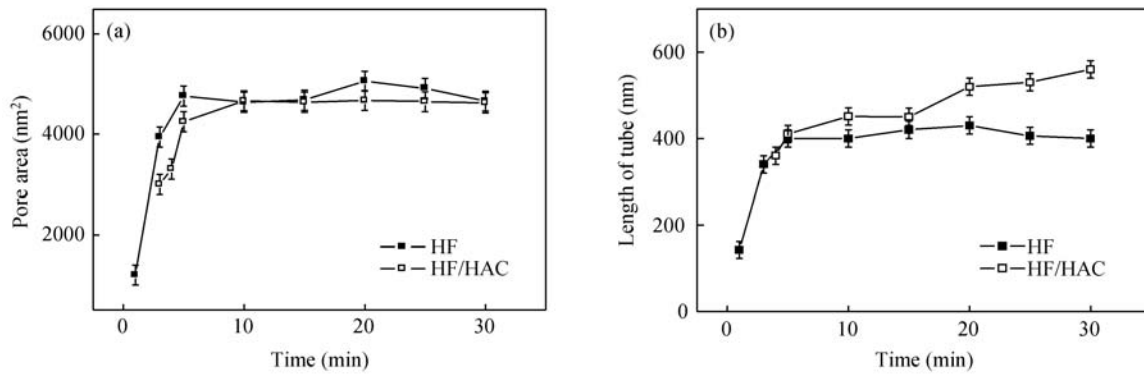
Fig. 6. Variation of the mean area of the pore mouth (a) and length of TiO_2 nanotubes (b) as a function of anodization time in 0.4 wt% HF electrolyte at 20 V with and without acid as the buffer medium in the anodization electrolyte.
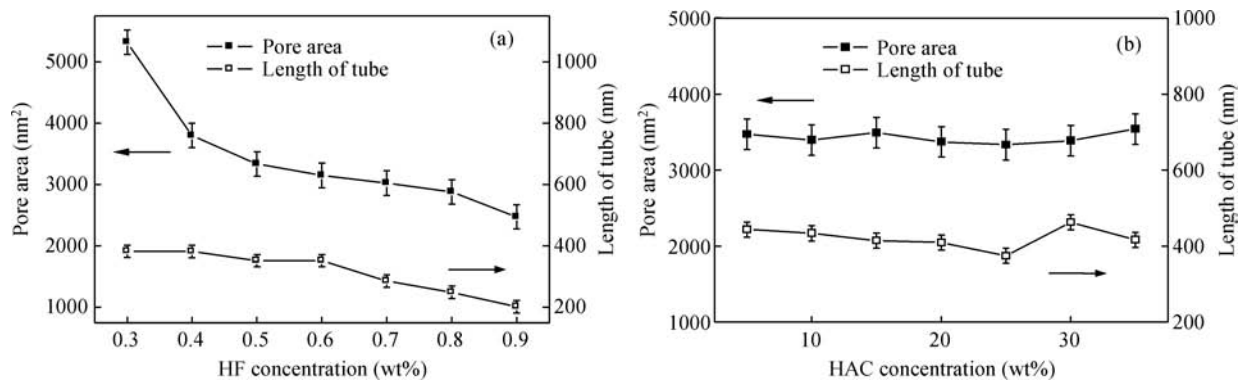

Fig. 7. (a) Variation of the mean area of the pore mouth and length of TiO_2 nanotubes as a function of HF concentration. (b) Mean area of the pore mouth and length of TiO_2 nanotubes as a function of HAC concentration in 0.4 wt% HF aqueous solution. The anodization voltage and time are 20 V and 15 min, respectively.

HF-containing electrolyte is shorter than that grown with HF/HAC in the electrolyte. TiO_2 nanotubes stop growing in both electrolytes after the anodization voltage is raised to higher than 18 V. It can easily be seen from Fig. 4 that the addition of acetic acid gives the TiO_2 nanotubes the chance to grow longer. The maximum TiO_2 nanotube length obtained is about 390 nm and 450 nm in HF and HF/HAC anodization electrolytes, respectively.

3.3. Effect of anodization time on the microstructure of TiO_2 nanotube arrays

Figure 6 summarizes the mean area of the pore mouth (Fig. 6(a)) and the length of TiO_2 nanotubes (Fig. 6(b)) as a function of anodization time in HF and HF/HAC electrolytes anodized at 20 V. The anodization duration dramatically affects the surface features of nanotubes for the first 5 min. Ordered TiO_2 nanotubes occur earlier in HF than in HF/HAC electrolytes. A longer anodization duration is helpful for the growth of longer TiO_2 nanotubes using HF/HAC electrolytes. The effect is, however, not obvious when HF electrolyte is used. Short and narrow TiO_2 nanotubes can be easily obtained with the use of HF electrolyte with short growth time. The maximum TiO_2 nanotube length reached 560 nm in HF/HAC electrolytes.

3.4. Effect of the electrolyte concentration on TiO_2 nanotube arrays

In Fig. 7(a), the mean area of the pore mouth and length of TiO_2 nanotubes are found to decrease dramatically with increasing HF concentration. When the concentration of HF is 0.3 wt%, the mean area of the pore mouth is about 5500 nm^2 and the length of the TiO_2 nanotubes is close to 400 nm; when the HF concentration is 0.9 wt%, the mean area of the pore mouth decreases to 2000 nm^2 and the length of the TiO_2 nanotubes to 200 nm. As mentioned above, the TiO_2 layer will break down when the H^+ concentration reaches certain level. A higher electrolyte concentration could provide more H^+ in the solution. With a high electrolyte concentration it is easy to gather enough H^+ at the bottom of the TiO_2 nanotubes when the TiO_2 nanotubes are relative small. Thus the mean area of the pore mouth and the length of TiO_2 nanotubes in a higher electrolyte concentration are relatively small. However, the mean area of the pore mouth and the length of TiO_2 nanotubes are essentially unchanged with the HAC concentration, as shown in Fig. 7(b).

The above results clearly indicate that anodization parameters play an important role in controlling the formation and geometric configuration of TiO_2 nanotubes by tuning the anodization voltage, electrolyte concentration, and anodization time.

4. Conclusion

In summary, we demonstrate the fabrication of TiO$_2$ nanotubes by constant voltage anodization of titanium foils in HF and HF/HAC electrolytes. The effect of anodization parameters on the diameter of nanotubes was also studied. TiO$_2$ nanotube arrays can be obtained by combining different anodization variables including anodization electrolyte concentration, anodization voltage, anodization time and buffer medium. The presence of HAC as a buffer medium can help grow longer TiO$_2$ nanotubes and more ordered microstructures.

References

[1] Doohun K, Andrei G, Sergiu P A, et al. Bamboo-type TiO$_2$ nanotubes: improved conversion efficiency in dye-sensitized solar cells. J Am Chem Soc, 2008, 130(49): 16454

[2] Kuang D, Brillet J, Chen P, et al. Application of highly ordered TiO$_2$ nanotube arrays in flexible dye-sensitized solar cells. ACS Nano, 2008, 2(6): 1113

[3] Varghese O K, Gong D, Paulose M, et al. Hydrogen sensing using titania nanotubes. Sensors and Actuators B, 2003, 93: 338

[4] Sergiu P A, Andrei G, Jan M M, et al. Self-organized, free-standing TiO$_2$ nanotube membrane for flow-through photocatalytic applications. Nano Lett, 2007, 7(5): 1286

[5] Rodriguez R, Kim K, Ong J L. In vitro osteoblast response to anodized titanium and anodized titanium followed by hydrothermal treatment. J Biomed Mater Res A, 2003, 65: 352

[6] Michailowski A, AlMawlawi D, Cheng G. Highly regular anatase nanotubule arrays fabricated in porous anodic templates. Chemical Physics Letter, 2001, 349: 1

[7] Chu S Z, Inoue S, Wada K, et al. A new electrochemical lithography: Fabrication of self-organized titania nanostructures on glass by combined anodization. J Electrochem Soc, 2005, 152: B116

[8] Masuda H, Kanezawa K, Nakao M, et al. Ordered arrays of nanopillars formed by photoelectrochemical etching on directly imprinted TiO$_2$ single crystals. Adv Mater, 2003, 15(2): 159

[9] Wijnhoven J E G J, Vos W L. Preparation of photonic crystals made of air spheres in titania. Science, 1998, 281: 802

[10] Chanmanee W, Watcharenwong A, Chenthamarakshan C R. Formation and characterization of self-organized TiO$_2$ nanotube arrays by pulse anodization. J Am Chem Soc, 2008, 130(3): 965

[11] Prakasam H E, Shankar K, Paulose M. A new benchmark for TiO$_2$ nanotube array growth by anodization. J Phys Chem C, 2007, 111(20): 7235

[12] Gong D, Grimes C A, Oomman K, et al. Titanium oxide nanotube arrays prepared by anodic oxidation. Journal of Materials Research, 2001, 16(12): 3331

[13] Paulose M, Prakasam H E, Oomman K, et al. TiO$_2$ nanotube arrays of 1000 μm length by anodization of titanium foil: phenol red diffusion. J Phys Chem C, 2007, 111(41): 14992

[14] Nageh K A, Craig A G. Formation of vertically oriented TiO$_2$ nanotube arrays using a fluoride free HCl aqueous electrolyte. J Phys Chem C, 2007, 111(35): 13028

[15] Yang Y, Wang X, Li L. Synthesis and growth mechanism of graded TiO$_2$ nanotube arrays by two-step anodization. Mater Sci Eng B, 2008, 149(1): 58

[16] Gerardo L, Christophe C, Alain J, et al. Nanostructured photovoltaic cell of the type titanium dioxide, cadmium sulfide thin coating, and copper thiocyanate showing high quantum efficiency. Chem Mater, 2006, 18(6): 1688

[17] Sun W, Yu Y, Pan H, et al. CdS quantum dots sensitized TiO$_2$ nanotube-array photoelectrodes. J Am Chem Soc, 2008, 130(4): 1124

[18] Macák J M, Tsuchiya H, Schmuki P. High-aspect-ratio TiO$_2$ nanotubes by anodization of titanium. Angew Chem Int Ed Engl, 2005, 44(14): 2100